The Effect of Particle Size on the Absorption of Cyclosporin A Nanosuspension Through the Gastrointestinal Barrier

Wenjun Sun
Academy of Military Medical Sciences Institute of Pharmacology and Toxicology
Jing Gao
Academy of Military Medical Sciences Institute of Pharmacology and Toxicology
Ranran Fan
Bengbu Medical College
Ting Zhang
Zhengzhou University
Yang Tian
Academy of Military Medical Sciences Institute of Pharmacology and Toxicology
Zengming Wang
Academy of Military Medical Sciences Institute of Pharmacology and Toxicology
Hui Zhang (zhhui58@126.com)
Academy of Military Medical Sciences Institute of Pharmacology and Toxicology
Aiping Zheng
Academy of Military Medical Sciences Institute of Pharmacology and Toxicology

Research

Keywords: Cyclosporin A nanosuspensions, Particle size, Transmembrane permeation, Situ single-pass intestinal perfusion, Pharmacokinetics

Posted Date: November 18th, 2021

DOI: https://doi.org/10.21203/rs.3.rs-1046785/v1

Abstract

Background: The particle size is one of great important properties of nanoparticles which affects the dissolution rate in vitro and pharmacokinetics in vivo. This study aimed to design an oral cyclosporin A nanosuspension (CsA-NS) and investigate the effect of particle size of cyclosporin A nanosuspension (CsA-NS) on absorption through the gastrointestinal barrier.

Results: CsA-NSs with different particle sizes were prepared. Dissolution rate in vitro, transmembrane permeation, gastrointestinal transport properties and the oral absorption of CsA-NSs were promoted by reducing size, except cellular uptake. Specially the particle size of CsA-NSs was nanoscale, their bioavailability was bioequivalent with marked soft capsules (Sandimmun Neoral®) which is self-microemulsion.

Conclusions: This study proposed the potential of developing CsA oral multi dosage form, taken the advantage of nanosuspensions.

Background

Cyclosporin A (CsA) is a lipophilic polypeptide of 11 amino acids with a molecular weight of 1202.61 g/mol, which is widely used as an immunosuppressant and anti-rejection drug in solid organ transplantation[1]. CsA is classified as BCS IV drugs (low solubility/low permeability) according to the biopharmaceutics classification system. Due to poor aqueous solubility (6.6 μg/ml) and poor intestinal permeability (p-glycoprotein substrates)[1,2], it is difficult to produce an oral formulation for CsA. There are two oral self-microemulsion formulations of CsA available, marketed as Sandimmune® and Neoral®, composed of a high concentration of polyoxyethylated castor oil (CremophorEL®, up to 38 w/w%)[3]. Especially, Neoral® shows relatively high therapeutic oral bioavailability with reduced variability. However, CremophorEL® has been identified as an unsafe oil composition that produces hypersensitivity, gastrointestinal, anaphylactoid, nephrotoxic and other adverse effects *in vivo*. Therefore, different strategies have been designed to develop an effective and safe oral formulation of CsA.

According to the Noyes-Whitney and Ostwald-Freundlich equations, reduction of particle size of drugs from micrometer to submicron or nanometer is one successful approach for improving solubility and enhancing dissolution rate of poorly soluble drugs[4,5]. Formulating poorly soluble drugs into nanosuspension is an effective method to improve oral bioavailability of insoluble drugs. Drug nanosuspensions are consist of pure drug particles with size rang 1000 nm to a few nm, and small amount stabilizers[6,7]. The particle size is one of great important properties of nanoparticles. It has been reported that the size of nanosuspensions can affect the dissolution rate in vitro and pharmacokinetics in vivo[8].

Currently, the most nanosuspensions drugs are oral administration on the market or in clinical research. The enhancement in oral bioavailability can be attributed to the increased solubility and dissolution rate

and improved bioadhesion of nanocrystals[9] as well as uptake of undissolved nanoparticle through enterocyte[8,10,11]. For example, the release rate and bioavailability of 160 nm betulinic acid nanosuspensions were higher than that of 400 nm and 700 nm betulinic acid nanosuspensions due to the increased solubility and dissolution rate[12]. The size also affects the efficiency and mechanism of cellular uptake[11,13]. Rejman[11,14] et al. investigated the effect of particle size on the pathway of entry in non-phagocytic B16 cells, the results showed that internalization of microspheres with a diameter < 200 nm involved clathrin-coated pits, for particles of 500 nm in size, caveolae-mediated internalization became predominant pathway of entry.

Compared with matrix nanoparticles, such as polymeric nanoparticles, liposomes and solid lipid nanoparticles, nanosuspensions offer almostly 100% drug loading[15] and reduced fasted/fed state variation[16,17]. Nanosuspensions also provide more options of dosage forms such as capsules and tablets or injection freeze-dried powder solidified by spray drying, freeze drying and fluidized bed drying, as well as better commercialization potential due to simple operation and easy industrial production of preparation methods[18,19].

Considering above factors, CsA was formulated into nanosuspensions. In the present study, CsA-NSs (Fig. 1.) were prepared by wet bead milling method with particle size of 280 nm, 522 nm and 2967 nm. The physical stability of particle size of CsA-NSs were investigated under simulated human gastrointestinal and cell culture conditions. Then the dissolution rates *in vitro* of CsA-NSs were investigated. The Caco-2 cell model was used for evaluating CsA-NSs absorption and transportation characteristics. The intestinal absorption properties of CsA-NSs were investigated by in situ single-pass intestinal perfusion model in SD rats. The absorption properties *in vivo* of CsA-NSs with different particle size were studied in SD rats.

Materials And Methods

Materials

Cyclosporin A (CsA) was purchased from Taishang Chemical Pharmacy Company (Taishang, China). Cyclosporin D (CsD) was purchased from Shanghai Tongtian Biotechnology Company (Shanghai, China). Neoral® (Ciclosporin soft gelatin capsules) was purchased from local drugstore. Vitamin E polyethylene glycol succinate (TPGS) was purchased from Shanghai Aladdin Biochemical Technology Co., Ltd. (Shanghai, China). Sodium dodecyl sulfate (SDS) were purchased from BASF, Ludwigshafen, Germany. Hydroxypropyl cellulose (HPC) was purchased from Nippon Soda Co., Ltd. (Tokyo, Japan). Simulated intestinal fluid (SIF) and simulated gastric fluid (SGF) were purchased from Shanghai yuanye Bio-Technology Co., Ltd. (Shanghai, China). Roswell Park Memorial Institute (RPMI) 1640 medium, phosphate buffered saline (PBS) and Hank's Balanced Salt Solution (HBSS) were purchased from HyClone Co., Ltd. (Utah, USA). Fetal bovine serum (FBS) was purchased from gibco Co., Ltd. (New York, USA). PMSF and RIPA buffer were purchased from Thermo Fisher Scientific Inc. (Illinois, USA). The purified water used in this study was prepared using a Mille-Q system

(EMD Millipore, Billerica, MA, USA). HPLC-grade acetonitrile and methanol were obtained from Thermo Fisher Scientific (Waltham, MA, USA). All other reagents were analytical grade.

Preparation of the CsA-NSs with Different Particle Sizes

CsA-NSs with different particle sizes were prepared by the wet bead milling method. HPC (7.5 g), TPGS (1.0 g) and SDS (0.1 g) were dissolved in deionized water (100 mL) to form a surfactant solution. CsA (15 mg) was added to the surfactant solution and stirred at 300 rpm with a magnetic agitator. The CsA suspensions and surfactant were processed with the high-pressure homogenization (HPH) technique by Ultra Turrax (T25; IKA, Staufen, Germany) at 10,000 rpm for 5 min, a uniform suspension was obtained. The uniform suspensions were then milled using the grinding machine (Dyno®-Mill Research Lab, WAB, Switzerland) at 1500, 2000, and 2500 rpm for 5 min, followed by 3000 rpm for 2.0 h to prepare CsA-NSs with the different particle sizes. The 0.3 mm yttrium-stabilized zirconium beads were used as milling media in this study.

Particle characterization

The mean particle size (MPS) and polydispersity index (PDI) of CsA-NSs with smaller particle sizes were detected by photon correlation spectroscopy (PCS), using a Malvern Zetasizer (ZS-90; Malvern Instruments, Malvern, UK). Potential larger particles or aggregates which cannot be detected by PCS. So, the median diameter (D_{50}) of CsA-NSs with larger particle sizes were analyzed by laser diffractrometry (LD) using a Mastersizer (2000; Malvern Instruments, Malvern, UK). Samples were diluted in water to a suitable concentration. The optical parameters of cyclosporin A were: real refractive index (RI) 1.49 and imaginary refractive index (IRI) 0.03[20]. D50 will also be referred to as MPS for ease of description in the following article.

Characterization of CsA-NSs with different particle sizes

The morphologies of CsA-NSs (280 nm), CsA-NSs (522 nm) and CsA-NSs (2967 nm) were determined by scanning electron microscopy (SEM) (JSM-7900F, JEOL, Japan) was used to determine morphologies of CsA-NSs. Samples were affixed to aluminum stubs using a double-sided carbon tape and sputter-coated with gold under an argon atmosphere. Differential scanning calorimetry (DSC) was performed with a DSC 214 differential scanning calorimeter (NETZSCH, Germany). The thermal properties of CsA, the excipients (HPC, TPGS and SDS), their physical mixture (raw CsA and stabilizers), and the CsA-NSs with different particle sizes were analyzed. Accurately weighted samples of 3 mg were placed in open aluminium pans, and DSC scans were recorded at a heating rate of 10 K/min from 20 ℃ to 200 ℃ under nitrogen purge gas flow (20 mL/min). An empty pan was used as reference. X-ray diffraction (XRD) was performed using a diffractometer (D8-Advance, Bruker, Germany) equipped with an Apex II CCD detector. The crystallinity state of CsA in raw CsA powder and CsA-NSs were analyzed. The X-ray source was Kα radiation from a copper target with a graphite monochromator at a wavelength of 1.54 Å. Standard runs using a 40 kV voltage, a 40- mA current, and a scanning rate of 2 °/min over a 2θ range of 5–45 ° were performed.

Particle size stability studies

This study aimed to investigate the effects of particle size on delivery of trans-intestinal epithelium transportation of CsA-NSs. So, it is necessary to investigate the stability of particle size in experimental process. The particle size of all the nanosuspensions were studied at 4 ℃ and room temperature. The particle size of CsA-NSs were also investigated in SGF, SIF, RPMI 1640 medium and HBSS. MPS and PDI of all samples were analyzed in triplicate and reported as the standard deviation.

The release of CsA-NS in vitro

A release study in vitro was carried out using the paddle method Chinese Pharmacopoeia specifications using a dissolution apparatus (RC1207DP, Tianda Tianfa Technology Co. Ltd., Tianjin, China). The CsA-NSs with different particle sizes containing an equivalent of 10 mg CsA were dropped into 900 mL of water, which was maintained at 37 ± 0.5 ℃ and stirred at 100 rpm. Samples (5 mL) were withdrawn and replaced with the equal volume of fresh medium at predetermined time intervals (5, 10, 20, 30, 40, 50, 60 min). The dissolution samples were filtered through a membrane filter of 0.22 μm pore size (Tianjin Jinteng Experimental Equipment, Co. Ltd., Tianjin, China). Apart from water, hydrochloric acid (pH 1.2), phosphate buffer (pH 4.5) and phosphate buffer (pH 6.8) were also respectively used as release mediums to investigate the release in vitro of CsA-NSs.

The content of CsA was assayed by a high-performance liquid chromatography (1640, Agilent, USA). The absorbance wavelength was set at 214 nm. The mobile phase was a mixture of phosphate acid (pH 1.2) solution and acetonitrile at a 10:90 v/v. A CAPCELL PAK C18 column (5 μm, 4.6 mm × 250 mm, Shiseido, Japan) was used with a flow rate of 1 mL/min and the column temperature was maintained at 70 ℃ using a column heater. The injection volume was 20 μL.

In vitro cellular uptake and Caco-2 monolayerpermeation

Cell culture

The Caco-2 cells were cultured by following the regular procedures in 1640 medium at 37 ℃, 90% RH and 5% CO_2 in T-25 flasks. The culture medium was changed every other day. The cells were passaged every 4-6 days after dissociation with 0.25% trypsin/0.02% EDTA solution when the cell fusion rate reached 85%.

In vitrocytotoxicity

Caco-2 cells were seeded in 96-well plates at a density of 5×10^4 cells in 200 μL medium per well and incubated for 48 h. The culture medium was removed, then culture medium containing various concentrations (from 200 to 400 μg/mL) of CsA-NSs with different particle sizes of 280 nm, 522 nm and 2967 nm were added to the cells. After 4 h, the medium was replaced with fresh medium containing 1 mg/mL of MTT, and the cells were further incubated for 4 h. Then the supernatant was removed, and the MTT formazan crystals were dissolved in 100 μL DMSO under gentle shaking for 30 min at room

temperature. The absorbance was measured using a Spectrophotometer (3020, Thermo Fisher Scientific Oy, USA) at 490 nm. Cell viability was calculated by measuring the absorbance.

Cellular uptakeof CsA-NS in Caco-2 cells

Caco-2 cells were seeded in 24-well plates at a density of 1×10^6 cells per well and incubated for 48 h to allow the cells to attach to the wells. The cells were treated with of 500 μL HBSS containing CsA -NSs (40 μg/mL CsA) for different time intervals. At certain time point, the HBSS was removed, and the cells were rinsed quintic with PBS, lysed with PMSF and RIPA buffer (PMSF: RIPA = 1:100).

Determination of CsA Concentration in the cell lysing reagent by LC/MS/MS.

Please refer to the Supplementary materials.

The result was expressed as the amount (μg) of drug per mg of total cellular protein.

Transport of CsA-NS across the Caco-2 cell monolayers

Caco-2 monolayers were used to evaluate the ability of transmembrane transportion for CsA-NSs. Briefly, Caco-2 cells were seeded onto the apical (AP) side of Millicell-CM cell culture plates (Millipore Corp., Bedford, MA, USA) in a density of 1×10^5 cells/cm^2, and cultured for 21 d under 5% CO_2, 90% relative humidity, and 37 ℃. The apical (AP) and basolateral (BL) compartments contained 0.5 and 1.5 mL of culture medium, respectively. The culture medium was replaced every other day for the first week and daily thereafter. The trans-epithelial electrical resistance (TEER) was measured, and a threshold value of 500 Ω/cm^2 was set for transmembrane studies. Prior to the experiments, the culture medium was replaced with warm HBSS (37 ℃). The cell monolayer was equilibrated at 37 ℃ for 30 min before conducting the transport studies. HBSS was removed and 200 μL HBSS containing CsA-NSs (40 μg/mL CsA) were added to the AP compartments, while 1.0 mL HBSS was filled into the BL side. At predetermined time points (0.5, 1.0, 1.5, 2, 2.5 and 3 h), aliquots (100 μL) were withdrawn from the BL side, and an equivalent volume of HBSS was added to maintain a constant volume. The CsA concentration in the samples was determined by LC-MS/MS. The preparation of the samples and LC-MS/MS conditions are detailed in "*In vitro* cellular uptake of CsA-NSs in Caco-2 cells". The apparent permeability coefficient (P_{app}, cm/s). P_{app} was calculated using the following equation[10]:

$$P_{app} = \frac{dQ}{dt} \times \frac{1}{AC_0}$$

where dQ/dt is the transport rate (μg/min), C_0 is the initial drug concentration on the apical side (μg/mL), and A is the surface area of the membrane filter (0.3 cm^{-2}).

Situ Single-Pass Intestinal Perfusion Experiments

Transport of CsA-NSs in the gastrointestinal (GI) tract was monitored by in situ single-pass intestinal perfusion experiments[21] (Fig.2). 15 male SD rats were randomly and equally divided into 3 groups: 280 nm-CsA-NS, 500 nm-CsA-NS and 2967 nm-CsA-NS. Cannulations were made at duodenum (1 to 11 cm downward from the pylorus), jejunum (15 to 25 cm downward from the pylorus), ileum (0 to 10 cm upward from the caecum) and colon (0 to 10 cm downward from the caecum) of anesthetized SD rats. The intestinal content was removed with physiological saline until the outlet solution appeared clear. CsA-NSs dilution (40 μg/mL CsA) were perfused along the bowel through the cannula at a flow rate of 0.20 mL/min to the intestinal segment. After a stabilization period of 30 min, perfusion fluid was collected into pre-weighed 5.0 mL vials every 20 min for 6 times. Samples were weighed and assayed by HPLC. The length of the intestinal segments was measured at the end of the experiment, and finally mercy killing of the animals were exercised. 200 μL acetonitrile was added into 50 μL of the sample followed by 1 min vortex mixing, then the sample was centrifuged at 14,500 × g for 10 min to obtain supernatant. At last, 20 μL supernatant was injected into HPLC to detect the concentration of CsA. HPLC conditions are detailed in "*In vitrorelease*".

The absorption rate constants (K_a) and effective permeability coefficients (P_{eff}) of CsA-NSs across rat intestine were calculated based on the disappearance of the drug in perfusate using the following equations[22].

$$K_{\alpha} = \frac{Q}{\pi r^2 L}\left(1 - \frac{C_{out}}{C_{in}} \times \frac{V_{out}}{V_{in}}\right)$$

$$P_{eff} = \frac{Q}{2\pi r L}\ln\left(\frac{C_{out}}{C_{in}} \times \frac{V_{out}}{V_{in}}\right)$$

where Q is the flow rate of the drug through the intestine (0.2 mL/min), r is the radius of the rat intestine, and L is the length of intestinal segment perfused after completion of the perfusion experiment. C_{in}, C_{out}, V_{in} and V_{out} are the drug concentration (μg/mL) and volume (mL) in the inlet of the perfusate entering the intestinal segment and the exiting solution, respectively.

Pharmacokinetic Studies

The *in vivo* pharmacokinetics of Neoral® microemulsion, CsA-NS (280 nm), CsA-NS (522 nm) and CsA-NS (2967 nm) were investigated. 20 healthy male SD rats were randomly divided into 4 groups (n = 5) and then administered with Neoral® microemulsion or CsA-NSs at an equivalent CsA dosage of 25 mg/kg via oral gavages. Orbital blood samples were collected at 0.25 h, 0.5 h, 1 h, 1.5 h, 2 h, 3 h, 4 h, 6 h, 8 h, 12 h, 24 h, 36 h and 48 h after administration using EDTA-K_2 surface-coated tubes, stored at −20 °C.

10 μL CsD (200 ng/mL) solution was added into 50 μL blood and then was vortex mixed for 30 s. 200 μL acetonitrile were added into the mixture and vortex-mixed for 1 min. Samples were then centrifuged at 14,000 × g for 10 min to obtain supernatant. Finally, the supernatant 5 μL were injected to determine the

CsA concentration in the whole blood using LC-MS/MS system. LC-MS/MS conditions are detailed in "*In vitro* cellular uptake of CsA-NSs in Caco-2 cells".

Data analysis

All results were expressed as mean ± SD. Statistical significance of the results was analyzed using one-way ANOVA. Values of $p < 0.05$ was considered statistically significant for all tests.

Results

Characterization of CsA-NS

Particle Size and Size Distribution

Particle Size of CsA-NSs were measured by DLS. As Figure 3 showed that the MPS becomes smaller and PDI becomes more uniform with prolongation of grinding time. Within 5 min, at a speed of 1500 rpm, MPS reduced to approx 3000 nm. With continuation of the milling, CsA-NSs with 500 nm and 280 nm were obtained after 30 min and 105 min at a speed of 3000 rpm, respectively. PDI ranged from 0.541 to 0.111. It was observed that the milling time more than 105 min could no longer decrease particle size.

Surface Morphology of CsA-NS

The morphology of CsA-NSs were observed under SEM. The scanning electron microscopy images are shown in Figure 4. CsA-NSs with particle size of 280 nm and 522 nm have near spheroid particle structures (A and B). Figure 2 (C) shows that CsA-NS with particle size of 2967 nm is irregular in shape.

Physical Status of CsA in the CsA -NS

Beside the size and distribution, the physical status of CsA in CsA-NSs is a very critical parameter. By using X-ray diffraction, we can analyze whether the crystalline form has changed in the preparation process. As shown in Figure 5, the original CsA has obvious diffraction peaks between 2θ values of 5° and 45°. This indicates that CsA exists in a crystalline state in raw CsA. The peaks of CsA in the physical mixture (raw CsA and stabilizers) became lower because it was probably bounded by the surfactant molecules. CsA-NSs show no diffraction peaks, due to amorphous structure caused by milling process and absolutely bounded by the surfactant molecules in the samples[23]. The XRD results confirm that CsA experienced crystalline transformation during the media milling process.

DSC thermograms of stabilizers, raw CsA, physical mixture (raw CsA and stabilizers), and powder of CsA-NSs are shown in Figure 6. The DSC thermogram of raw CsA shows a weak endothermic peak at approximately 107–132 °C[24]. It means there is some CsA of crystalline state in raw CsA. The peak of pure CsA was not observed in the thermogram of the physical mixture, which shew obvious influence from stabilizers. In the CsA-NSs with different particle size of 280 nm, 522 nm and 2967 nm, this peak was also not present, but the DSC thermograms showed a gentle exothermic peak at approximately

80 ℃, which presents crystallization process and indicates that CsA occurs in an amorphous form in CsA-NSs. The DSC thermograms of stabilizers and physical mixture show sharp transitions at 37 ℃, which correspond to the melting points of TPGS (37–41 ℃)[25],but this peak is absent in the freeze-dried CsA-NSs, it can been concluded that TPGS was absorbed by the surface of nanoparticles in molecular form.

Particle size stability studies

It is important that the CsA-NS remains stable in different condition. Especialy, for nanoparticle, particle size is one of most important indexes. As shown in Figure 7, no significant changes in MPS of the CsA-NSs could be observed within three months 4 ℃ and room temperature (RT), indicating that the particle size of CsA-NSs is sufficiently stable in storage. The particle size of the CsA-NSs increases only slightly after the CsA-NSs were mixed with HBSS, 1640 culture, SGF and SIF at 37 ℃ for 4 h, 4 h, 2 h and 12 h, respectively, which suggests that they could remain stable in the whole experiments cycle.

In vitro dissolution of CsA-NS

The release profiles of CsA-NSs with different particle size were evaluated in four kinds of medium: water, hydrochloric acid pH 1.2, phosphate buffer pH 4.5 and phosphate buffer pH 6.8. As shown in Figure 8A, the CsA-NSs with smaller particle size showed higher dissolution rate in comparison to CsA-NSs with larger particle size in water. CsA-NSs (280 nm) released more than 90% of CsA within 20 min. The release percentage of CsA from the CsA-NS (522 nm) and CsA-NS (2967 nm) were approximately 85% and 70% within 40 min, respectively. The same release trend also occurs in other medium, hydrochloric acid pH 1.2 (Figure 8B), phosphate buffer pH 4.5 (Figure 8C) and phosphate buffer pH 6.8 (Figure 8D).

Cytotoxicity

The cytotoxic effects of CsA-NSs with different particle sizes were evaluated in the Caco-2 cell line. As shown in Figure 9, there was no significant differences in cell viability compared with the control, when the CsA concentrations in cell medium were lower than 200 μg/mL. When the CsA concentration of CsA-NS (2967 nm) or CsA-NS (522 nm) in cell medium was 400 μg/mL or 600 μg/mL respectively, the cell viability was significantly different from the control group. This suggested that CsA-NSs with a larger particle size (522 nm and 2967 nm) were more toxic to Caco-2 cell.

Cellular Uptake Studies

To study the bioavailability potential of the CsA-NSs for oral delivery, it is important to understand the effect of particle size on the cellular uptake of Caco-2 cells. As shown in Figure 10, the cellular uptake of all CsA-NSs increased during the whole incubation stage from 0.5 to 2 h. The cellular uptake of CsA-NSs in Caco-2 cells reduced with particle size increasing, this was consistent with the result of the previous toxicity test. After 2 h incubation with CsA-NS (2967 nm), the cells contained 4409 ng CsA per mg of

protein, while 4202 and 3846 ng CsA per mg of protein for CsA-NS (522 nm) and CsA-NS (280 nm) respectively.

Transport of CsA-NSs across the Caco-2 cell monolayers

To evaluate the transmembrane capacity of CsA-NSs with different particle size, we determined the amount of CsA transporting across Caco-2 cell monolayers from the AP side to the BL side. In all the experiments, the TEER values showed no changes,which indicates there is no cellular monolayers damage during experiment. Relative cumulative transport of CsA in CsA-NSs across Caco-2 cell monolayers from the apical to the basolateral side after 3 h of incubation at 37 ℃ were shown in Figure 11A. The amount of CsA in the BL side of monolayers treated with CsA-NS (280 nm) is highest among the three kinds of CsA-NSs with different particle size at each time point. After 3h incubation, the relative cumulants of CsA in the BL side was 4.18%, 3.88% and 2.98% for NS (280 nm), NS (522 nm) and NS (2967 nm) respectively. These results indicate that the relative cumulative transport of CsA increased with the decrease of particle size and the extension of time in the BL side.

The P_{app} of CsA from the apical side to the basolateral side was calculated after incubating Caco-2 cells with CsA-NSs for 0 to 3.0 h. As shown in Figure 11B, the P_{app} of the CsA-NSs of 280 nm [(11.73±5.35) $\times10^{-6}$ cm/s] was higher than the corresponding value of CsA-NS of 522 nm [(10.84±1.79) $\times10^{-6}$ cm/s], and significantly higher than the corresponding value of CsA-NS of 2967 nm [(8.363±4.46) $\times10^{-6}$ cm/s].

In situ perfusion

In the intestinal absorption studies, the absorption characteristics of CsA-NSs with different size were assessed in four segments of small intestine from alive SD rats: duodenum, jejunum, ileum and colon. The absorption rate constants (K_a) and effective permeability coefficients (P_{eff}) obtained in the single-pass intestinal perfusion (SPIP) models are presented in Table 1. The K_a and P_{eff} of CsA-NS (280 nm) are all the highest in four segments. In addition, CsA-NSs absorption in duodenal absorption is the best, followed by ileum and jejunum, finally colon. In duodenal, K_a of CsA-NS (280 nm) [(5.454±0.5249)$\times10^{-2}$ min^{-1}] was significantly higher than K_a of CsA-NS (522 nm) [(4.605±0.5684)$\times10^{-2}$ min^{-1}] and K_a of CsA-NS (2967 nm) [(3.267±0.9684) $\times10^{-2}$ min^{-1}]. And P_{eff} of CsA-NS (280 nm) [(5.784±0.6385) $\times10^{-3}$ cm· min^{-1}] was significantly higher than P_{eff} of CsA-NS (2967 nm) [(3.295±0.1354) $\times10^{-3}$ cm· min^{-1}]. Similar results occurred in other intestinal segments. For CsA-NS (280 nm), K_a in duodenal was significantly higher than K_a [(3.682±0.9481) $\times10^{-2}$ min^{-1}] in jejunum and K_a [(3.682±0.9481) $\times10^{-2}$ min^{-1}] in colon. And P_{eff} in duodenal was significantly higher than P_{eff} [(3.064±0.3239) $\times10^{-2}$ min^{-1}] in colon. Similar results occurred for CsA-NS (522 nm) and CsA-NS (2967 nm).

Table 1. Absorption parameters of CsA-NSs in different regional intestines studied with different size at a dose of 40 μg/mL (n =5, means ± s)

Size / nm	Segments of rat intestine	Parameter	
		$K_a \times 10^{-2}$/ min^{-1}	$P_{eff} \times 10^{-3}$ / $cm \cdot min^{-1}$
280	Duodenum	5.454±0.5249 b, cc, 22, 44	5.784±0.6385 cc, 44
	Jejunum	3.682±0.9481 c, 11, 44	4.321±1.634 c, 44
	Ileum	4.6944±1.240 c, 44	4.335±1.588 c, 44
	Colon	2.216±0.1683 cc, 11, 22, 33	3.064±0.3239 cc, 11, 22, 33
522	Duodenum	4.605±0.5684 a, c, 2, 44	5.044±1.207 c, 2, 44
	Jejunum	3.778±0.4680 c, 1, 44	3.745±0.3123 c, 1, 4
	Ileum	3.903±0.6299 c, 44	3.882±1.142 c, 4
	Colon	2.253±0.7191 c, 11, 22, 33	2.768±0.5846 c, 11, 2, 3
2967	Duodenum	3.267±0.9684 aa, b, 44	3.295±0.1354 aa, b, 4
	Jejunum	2.430±0.3816 a, b, 4	2.054±0.6317 a, b
	Ileum	2.796±0.4874 a, b, 44	2.499±0.7047 a, b, 4
	Colon	1.614±0.2887 aa, b, 11, 2, 33	1.727±0.3964 aa b, 1, 3

Note: a, b and c represent significantly different compared with 280 nm, 522 nm and 2967 nm CsA-NSs, respectively ($p < 0.05$); aa, bb and cc represent extremely significant different compared with 280nm, 522 nm and 2967 nm CsA-NS, respectively ($p < 0.01$); 1, 2, 3 and 4 represent significantly different compared with duodenum, jejunum, ileum and colon, respectively ($p < 0.05$); 11, 22, 33 and 44 represent represent extremely significant different compared with duodenum, jejunum, ileum and colon, respectively ($p < 0.01$).

Pharmacokinetics Studies

In pharmacokinetic studies of CsA-NSs after oral administration, SD rats were selected as model animals. The blood concentration–time profiles of CsA are shown in Figure 12, and the pharmacokinetic parameters are shown in Table 2. The results revealed that, CsA-NS (280 nm) showed the highest C_{max} (2.364±0.289 μg/mL) of CsA at T_{max} of 4.2±2.1 h in the three kinds of CsA-NSs, while CsA-NSs with size of 2967 nm showed the lowest (1.546 ± 1.021 μg/mL) at T_{max} of 5.8 ± 2.2 h. And, in case of CsA-NS with size of 522 nm, the C_{max} of CsA was found to be 2.364±0.289 μg/mL at 4.3±3.4 h. Furthermore, the $AUC_{0\text{-}48h}$ of 280 nm CsA-NS was about 1.12-fold of that 522 nm CsA-NS, and about 1.51-fold of that 2967 nm CsA-NS.

The $AUC_{0\text{-}48h}$ of 280 nm, 522 nm and 2967 nm CsA-NSs were compared with the reference (Neoral®) values, resulting in a relative bioavailability of 90.20%, 80.18% and 59.61%, respectively. It was evident that, the $AUC_{0\text{-}48h}$ and C_{max} values of CsA-NSs formulations increased in descending order: 280 nm > 522 nm > 2967 nm, while the T_{max} values followed the reverse rank order for the different sized samples.

Table 2. Pharmacokinetic parameters of Neoral® and different sized CsA-NSs at a dose of 25 mg/kg in SD rats (n = 5, means ± s).

Group	C_{max} (μg/mL)	T_{max} (h)	$AUC_{0\text{-}48h}$ (h*μg/mL)	Frel (%)
280 nm	2.364±0.289§	4.2±2.1	57.245±0.915§	90.20
522 nm	1.991±0.147*	4.3±3.4	50.886±0.776§	80.18
2967 nm	1.546 ± 1.021#*	5.8 ± 2.2*	37.831±4.465*#□	59.61
Neoral®	2.942±0.956□§	4.0 ± 2.3§	63.461±13.996§	

Note: *, #, □, § represent significantly different compared with Neoral®, 280 nm, 522 nm and 2967 nm CsA-NS, respectively ($p < 0.05$).

Abbreviations: C_{max}, maximum whole blood concentration; T_{max}, time to reach maximum whole blood concentration; AUC, area under the whole blood concentration, Frel, relative oral bioavailability.

Discussion

In the present study, CsA-NSs with different particle sizes were prepared. Extension of the milling time can obviously reduce the particle diameter within 105 min. And CsA-NS with the smallest particle size 280 nm was obtained. But in this study, if the milling time is over 105 min, the particle size could no longer decrease, conversely, the particle size of CsA-NSs increased. A similar phenomenon as above has been seen in other studies[26]. Thus, for CsA-NSs in this study, the diameter of 280 nm is probably minimum lower limit. It's reported that the upper size limit of nanoparticle internalized into non-phagocytotic cells by means of nonspecific endocytosis was 3000 nm[27], and the nanoparticle of 3000 nm also can be adsorbed and immobile within the submucosal layer of the thicker mucosa and the Peyer's patches[28]. For 500 nm particles, many researches confirmed that it can be absorbed by Peyer's patches in intestine and found absorption maximum among particles between 100 nm and 3 μm[11,28]. So, the CsA-NSs with size of 280 nm, 522 nm and 2967 nm were applied to the following research process.

This study aimed to investigate the effects of particle size on trans-intestinal epithelium transportation of CsA-NSs. It is necessary to investigate the particle size stability of CsA-NSs in different conditions involved in the experiments. As shown in Figure 7, the particle size of CsA-NSs has no significantly change in storage and remain stable in the whole experiments. In dissolution study, the release rate of CsA-NS (280 nm) was the fastest, and the cumulative drug release was the highest. These results indicated that the drug release or dissolution rate from CsA-NSs followed a particle size dependent dissolution trend. The increased rate of drug release is likely due to the small size and large surface area of CsA-NSs, as predicted by the Noyes–Whitney equation.

Caco-2 cells derived from a colon carcinoma and can mimic successfully a biological barrier, which also possess high levels of p-glycoprotein. Given gastrointestinal condition, especially a high expression of p-glycoprotein in the lower GI-tract and colon, Caco-2 cells were used to evaluate the cellular uptake, in this study. The cellular uptake gradually increased during the whole incubation stage from 0.5 to 2 h. Furthermore, the increase range of cellular uptake for CsA-NSs with a larger particle size was higher (Fig 10.), which is consistent with the toxicity test (Fig 9.). These results conflict with other reported research[29,30], in which the cell uptake of microparticle is dependent upon the particle size, the smaller particles are, the greater uptake they have[31]. We analyzed the reasons of the phenomenon appealing from the following aspects (Fig 13.). Firstly, as a classical transported substrate of p-glycoprotein, CsA can be secreted from the Caco-2 cells by p-glycoprotein[32]. Secondly, the smaller size microparticles < 200 nm were mostly localized in the lysosomals[14,33], where CsA can be metabolized partly. Thirdly, smaller nanoparticles can penetrate cell easier by transcellular transportation including the endocytosis and exocytosis of nanoparticles[34-37]. Although the internalization of 2967 nm CsA-NS might be less, as compared with 280 nm and 522 nm, actual CsA in whole cell might well be higher due to lower effluent, degradation and exocytosis. In this work, we find that the efficiency of cellular uptake depends on not only particle size but also drug properties. For other drug and cell types, particle size-dependent endocytosis may not be the rate limiting step in cellular uptake efficiency, and more parameters should be

considered for in cell studies. These results are limited to cellular uptake study, and the ultimate absorption through the gastrointestinal barrier needs been characterized by transmembrane transport and in vivo pharmacokinetics.

After 20-21 days culture，the Caco-2 cells formed enterocyte-like cell monolayer and expressed tight junction, micro villi and brush border[22]. The Caco-2 cell monolayers, a good model for intestinal epithelium, could be used prior to in vivo studies for a rapid assessment of the factors. No significant differences in TEER values of cell monolayers was observed before and after experiments, which demonstrated the unchanged integrity of cell monolayers[38]. Cumulative transport of CsA-NSs across Caco-2 cell monolayers from the apical to the basolateral side after 3 h incubation at 37°C is shown in Figure 8. Our results show that the concentration of CsA in the basolateral side increased with the decrease of particle size and the extension of time. The increase of dissolution rate and saturation solubility caused by the decrease of particle size are responsible for improving transport of CsA through caco-2 cell monolayer. Meanwhile, nano-particles with smaller size also appeared to across from apical to basolateral monolayer more than the larger ones[35]. Though p-glycoprotein presenting in Caco-2 cell inhibits the overall permeation of CsA, the transport system back into the apical lumen becomes saturated and the diffusion rate through the cells monolayer is the overall limiting factor at higher concentrations[32]. Therefore, reducing particle size and increasing solubility is one of the effective means to increase cells monolayer transport.

Compared with Caco-2 models, the in-situ perfusion models address the complexity of intestinal processes, which eventually determine in vivo intestinal absorption. These complexity not only includes normal expression levels of P450 enzymes and existence of a protective mucus layer[39], but also remains intact blood vessels and nerves[40]. The obtained assessment is based on the disappearance of the drug in the lumen. The results show the K_a and P_{eff} appeared to be higher with the particle size of CsA-NSs decrease. This is because that the transport of CsA-NSs across intestine could be stimulated by improving dissolution rate and saturation solubility, prolonging the time of mucoadhesion to GI[41], as well as adsorptive endocytosis caused by the decrease of particle. In addition, the results also show that CsA-NSs in duodenal absorption is the best, followed by it is ileum and jejunum, finally colon. The reasons for this result are complex (Fig 14.). Firstly, there are lower effusion and higher metabolism of CsA because of less p-glycoprotein[32,42] and more CYP 3A9 (metabolic enzymes of CsA)[4339]{Wu, 2019 #34;!!! INVALID CITATION !!! , #0;Cao X, 2006 #51} in duodenal compared with other intestinal segments. Secondly, various digestive juices, such as bile (bile salt, bile pigment, cholesterol, lecithin and so on), enter the small intestine through the duodenal segment. The bile could act as surfactant to promote the dissolution and absorption of CsA-NSs. And the cholesterol involved in particle endocytosis, the absorption of nanoparticles in the duodenum is further promoted. Due to the special physiological characteristics of the duodenum leading to high metabolism, low effusion, high solubility, and efficient particle endocytosis, the disappearance of CsA in the CsA-NSs perfusion fluids with different particle sizes was the largest in the duodenum. It's reported that ileum carries more Peyer's patches and M cells

than jejunum, in which particles above 1 μm can be trapped in Peyer's patches[35,44]. This may be the reason why more CsA-NSs is absorbed in ileum than jejunum.

The pharmacokinetics of CsA-NSs with different particle sizes following a dose oral administration of 25 mg/kg was investigated in SD rats using the marketed microemulsion (Neoral®) as reference. Mean drug plasma concentration-time profiles and pharmacokinetic parameters of CsA-NSs are showed in Figure 11 and Table 2. CsA-NS (280 nm) exhibits more desirable pharmacokinetic characteristics compared to CsA-NS (522 nm) and CsA-NS (2967 nm). The $AUC_{0\text{-}48h}$ and C_{max} values of CsA-NSs formulations increased in descending order of 280 nm > 522 nm > 2967 nm, while the T_{max} values followed the reverse rank order for the different sized samples. These results could be attributed to the increased saturation solubility and dissolution velocity in digestive juice as well as prolonging time of mucoadhesion to GI of CsA-NSs caused by the decrease of particle[45]. Moreover, integral nanocrystals across gastrointestinal barrier (GI) entered systemic circulation via several mechanisms, include paracellular passage (size < 50 nm), endocytosis uptake (size < 500 nm) and the lymphatic uptake (size < 5,000 nm) - particles adsorbed by the M cells of the Peyer's patches[29]. It means that integral CsA-NSs with smaller size have more ways into systemic circulation across GI. Pharmacokinetic data show that the smaller particle size, the higher the oral bioavailability of CsA-NSs, which is consistent with the results of transport across the Caco-2 cell monolayers and situ single-pass intestinal perfusion experiments and demonstrated that most of the drug reduced during situ single-pass intestinal perfusion experiments was absorbed into the blood. Compared with the commercially available drug Neroal®, the relative bioavailability of CsA-NS (280 nm) can reach 90.2%. This indicates that CsA-NS (280 nm) is bioequivalent to and substitutable with the commercially available drug Neroal®.

Conclusion

In the present study, CsA-NSs with particle sizes of 280 nm, 522 nm and 2967 nm were prepared by wet bead milling method. The particle size had a significant influence on the dissolution behavior, cytotoxicity and cellular uptake in Caco-2 cells, transmembrane permeation across Caco-2 cell monolayers, transport properties in the small intestine and pharmacokinetics properties in SD rats of CsA-NSs. The potential of CsA-NSs with smaller particle size were appealing. This study will provide guidance for novel dosage forms of CsA.

Abbreviations

CsA-NS, cyclosporin A nanosuspension; CsA, cyclosporin A; BCS , biopharmaceutics classification system; CsD, cyclosporin D; TPGS, vitamin E polyethylene glycol succinate; SDS, sodium dodecyl sulfate; HPC, Hydroxypropyl cellulose; SIF, simulated intestinal fluid; SGF, simulated gastric fluid; 1640 medium, Roswell Park Memorial Institute 1640 medium; PBS, phosphate buffered saline; HBSS, Hank's Balanced Salt Solution; DMSO, dimethyl sulfoxide; FBS, fetal bovine serum; MPS, mean particle size; SEM, scanning electron microscope; DSC, differential scanning calorimeter; PCS, photon correlation spectroscopy; D50,

median diameter; PDI, polydispersity; HPH, high-pressure homogenization; LD, laser diffractometry; RI, real refractive index; IRI, imaginary refractive index; TEER, trans-epithelial electrical resistance; GI, gastrointestinal; SD rat, Sprague–Dawley rat; RH, relative humidity; TEM, transmission electron microscopy; XRD, X-ray diffraction; SD, standard deviation; C_{max}, maximum whole blood concentration; T_{max}, time to reach maximum whole blood concentration; AUC, area under the whole blood concentration, Frel, relative oral bioavailability

Declarations

Ethics approval and consent to participate

Male Sprague–Dawley rats weighing 200–250 g (certificate no. SCXK- (Beijing) 2018-0010) were provided by the Beijing Institute of Pharmacology and Toxicology (Beijing, China). The pharmacokinetics study was approved by the Animal Ethics Committee at Beijing Institute of Pharmacology and Toxicology (ethics code permit no. IACUC-DWZX-2020-639). Moreover, approval was received prior to beginning this research.

Consent for publication

Not applicable

Availability of data and materials

The datasets used and/or analyzed during the current study are available from the corresponding author on reasonable request.

Competing interests

The authors declare that they have no competing interests.

Funding

This work was supported by National Natural Science Foundation of China (No. 81573357).

Author Contributions

WS, AZ and HZ designed the project. WS, RF and TZ performed the experiments. JG and ZW provided consulting services. WS and AZ acquired, analyzed and interpreted the data. WS, HZ and YT drafted the manuscript. HZ critically revised the manuscript. All of the authors have read and approved the final manuscript.

Acknowledgements

Not applicable

References

1 Jain, S., Kambam, S., Thanki, K. & Jain, A. K. Cyclosporine A loaded self-nanoemulsifying drug delivery system (SNEDDS): implication of a functional excipient based co-encapsulation strategy on oral bioavailability and nephrotoxicity. *RSC Advances***5**, 49633-49642, doi:10.1039/c5ra04762e (2015).

2 Basaran, E., Demirel, M., Sirmagul, B. & Yazan, Y. Cyclosporine-A incorporated cationic solid lipid nanoparticles for ocular delivery. *J Microencapsul***27**, 37-47, doi:10.3109/02652040902846883 (2010).

3 Liu, M., Zhong, X. & Yang, Z. Chitosan functionalized nanocochleates for enhanced oral absorption of cyclosporine A. *Sci Rep***7**, 41322, doi:10.1038/srep41322 (2017).

4 Kesisoglou, F., Panmai, S. & Wu, Y. Nanosizing–oral formulation development and biopharmaceutical evaluation. *Adv Drug Deliv Rev***59**, 631-644, doi:10.1016/j.addr.2007.05.003 (2007).

5 Du, B. *et al.* Development and characterization of glimepiride nanocrystal formulation and evaluation of its pharmacokinetic in rats. *Drug Deliv***20**, 25-33, doi:10.3109/10717544.2012.742939 (2013).

6 Muller, R. H., Gohla, S. & Keck, C. M. State of the art of nanocrystals–special features, production, nanotoxicology aspects and intracellular delivery. *Eur J Pharm Biopharm***78**, 1-9, doi:10.1016/j.ejpb.2011.01.007 (2011).

7 Kayaert, P. *et al.* Solution calorimetry as an alternative approach for dissolution testing of nanosuspensions. *Eur J Pharm Biopharm***76**, 507-513, doi:10.1016/j.ejpb.2010.09.009 (2010).

8 Lu, Y. e. a. The in vivo fate of nanocrystals. *Drug Discov Today***22**, 744-750, doi:10.1016/j.drudis.2017.01.003 (2017).

9 Li, Q., Liu, C. G. & Yu, Y. Separation of monodisperse alginate nanoparticles and effect of particle size on transport of vitamin E. *Carbohydr Polym***124**, 274-279, doi:10.1016/j.carbpol.2015.02.007 (2015).

10 He, Y., Xia, Dn., Li, Qx. et al. Enhancement of cellular uptake, transport and oral absorption of protease inhibitor saquinavir by nanocrystal formulation. *Acta Pharmacol Sin***36**, 1151-1160, doi:10.1038/aps.2015.53 (2015).

11 Xie, Y. *et al.* Epithelia transmembrane transport of orally administered ultrafine drug particles evidenced by environment sensitive fluorophores in cellular and animal studies. *J Control Release***270**, 65-75, doi:10.1016/j.jconrel.2017.11.046 (2018).

12 Wang, R., Wang, X., Jia, X., Wang, H. & Li, J. Impacts of particle size on the cytotoxicity, cellular internalization, pharmacokinetics and biodistribution of betulinic acid nanosuspensions in combined chemotherapy. *International Journal of Pharmaceutics***588**, 119799 (2020).

13 Langston Suen, W. L. & Chau, Y. Size-dependent internalisation of folate-decorated nanoparticles via the pathways of clathrin and caveolae-mediated endocytosis in ARPE-19 cells. *J Pharm Pharmacol***66**, 564-573, doi:10.1111/jphp.12134 (2014).

14 Rejman, J., Oberle, Zuhorn, I. & Hoekstra, D. Size-dependent internalization of particles via the pathways of clathrin- and caveolae-mediated endocytosis. *Biochemical Journal***377**, 159-169 (2004).

15 Bi, C. *et al.* Particle size effect of curcumin nanosuspensions on cytotoxicity, cellular internalization, in vivo pharmacokinetics and biodistribution. *Nanomedicine***13**, 943-953, doi:10.1016/j.nano.2016.11.004 (2017).

16 Zhang, X. *et al.* Exploration of nanocrystal technology for the preparation of lovastatin immediate and sustained release tablets. *Journal of Drug Delivery Science and Technology***50**, 107-112, doi:10.1016/j.jddst.2019.01.018 (2019).

17 Zhang, X., Li, L. C. & Mao, S. Nanosuspensions of poorly water soluble drugs prepared by top-down technologies. *Curr Pharm Des***20**, 388-407, doi:10.2174/13816128113199990401 (2014).

18 Jacob, S., Nair, A. B. & Shah, J. Emerging role of nanosuspensions in drug delivery systems. *Biomater Res***24**, 3, doi:10.1186/s40824-020-0184-8 (2020).

19 Pawar, V. K., Singh, Y., Meher, J. G., Gupta, S. & Chourasia, M. K. Engineered nanocrystal technology: in-vivo fate, targeting and applications in drug delivery. *J Control Release***183**, 51-66, doi:10.1016/j.jconrel.2014.03.030 (2014).

20 Romero, G. B., Arntjen, A., Keck, C. M. & Muller, R. H. Amorphous cyclosporin A nanoparticles for enhanced dermal bioavailability. *Int J Pharm***498**, 217-224, doi:10.1016/j.ijpharm.2015.12.019 (2016).

21 Ding, W. *et al.* Co-delivery of honokiol, a constituent of Magnolia species, in a self-microemulsifying drug delivery system for improved oral transport of lipophilic sirolimus. *Drug Delivery*, 1-11 (2016).

22 Cummins, C. L., Salphati, L., Reid, M. J. & Benet, L. Z. In Vivo Modulation of Intestinal CYP3A Metabolism by P-Glycoprotein: Studies Using the Rat Single-Pass Intestinal Perfusion Model. *Journal of Pharmacology and Experimental Therapeutics***305**, 306-314 (2003).

23 Rahman, Z. *et al.* Characterization of 5-fluorouracil microspheres for colonic delivery. *AAPS PharmSciTech***7**, E47, doi:10.1208/pt070247 (2006).

24 Guada, M., Lasa-Saracibar, B., Lana, H., Dios-Vieitez Mdel, C. & Blanco-Prieto, M. J. Lipid nanoparticles enhance the absorption of cyclosporine A through the gastrointestinal barrier: In vitro and in vivo studies. *Int J Pharm***500**, 154-161, doi:10.1016/j.ijpharm.2016.01.037 (2016).

25 Mu, L. & Feng, S. S. Vitamin E TPGS used as emulsifier in the solvent evaporation/extraction technique for fabrication of polymeric nanospheres for controlled release of paclitaxel (Taxol). *Journal of Controlled*

*Release***80**, 129-144 (2002).

26 Jog, R. & Burgess, D. J. Comprehensive Quality by Design Approach for Stable Nanocrystalline Drug Products. *International Journal of Pharmaceutics* (2019).

27 Gratton, S. E. *et al.* The effect of particle design on cellular internalization pathways. *Proc Natl Acad Sci U S A***105**, 11613-11618, doi:10.1073/pnas.0801763105 (2008).

28 Jani, P., Halbert, G. W., Langridge, J. & Florence, A. T. Nanoparticle Uptake by the Rat Gastrointestinal Mucosa: Quantitation and Particle Size Dependency. *Journal of Pharmacy and Pharmacology***42** (1990).

29 Kulkarni, S. A. & Feng, S. S. Effects of Particle Size and Surface Modification on Cellular Uptake and Biodistribution of Polymeric Nanoparticles for Drug Delivery. *Pharmaceutical Research***30**, 2512 (2013).

30 Olejnik M, K. M., Rosenkranz N. et al. Cell-biological effects of zinc oxide spheres and rods from the nano- to the microscale at sub-toxic levels. *Cell Biology and Toxicology* (2020).

31 Salatin, S., Dizaj, S. M. & Khosroushahi, A. Y. Effect of the surface modification, size, and shape on cellular uptake of nanoparticles. *Cell Biology International***39** (2015).

32 Fricker, G., Drewe, J., Huwyler, J., Gutmann, H. & Beglinger, C. Relevance of p-glycoprotein for the enteral absorption of cyclosporin A: in vitro-in vivo correlation. *British Journal of Pharmacology***118**, 1841-1847 (2012).

33 Rennick, J. J., Johnston, A. P. R. & Parton, R. G. Key principles and methods for studying the endocytosis of biological and nanoparticle therapeutics. *Nat Nanotechnol***16**, 266-276, doi:10.1038/s41565-021-00858-8 (2021).

34 Jenkins, P. G. e. a. Microparticulate absorption from the rat intestine. *Journal of Controlled Release***29**, 339-350 (1994).

35 Witoonsaridsilp, W., Panyarachun, B., Jaturanpinyo, M. & Sarisuta, N. Phospholipid vesicle–bound lysozyme to enhance permeability in human intestinal cells. *Pharmaceutical Development & Technology***18**, 821-827 (2013).

36 Chithrani, B. D. & Chan, W. C. Elucidating the mechanism of cellular uptake and removal of protein-coated gold nanoparticles of different sizes and shapes. *Nano Lett***7**, 1542-1550, doi:10.1021/nl070363y (2007).

37 Kristin Denzer, M. J. K., Harry F. G. Heijnen, Willem Stoorvogel and Hans J. Geuze. <Exosome from internal vesicle of the multivesicular body to intercellular signaling device.pdf>. *Journal of Cell Science***113**, 3365-3374 (2000).

38 Chen, T. *et al.* Oral Delivery of a Nanocrystal Formulation of Schisantherin A with Improved Bioavailability and Brain Delivery for the Treatment of Parkinson's Disease. *Molecular Pharmaceutics*, acs.molpharmaceut.6b00644 (2016).

39 Stappaerts, J., Brouwers, J., Annaert, P. & Augustijns, P. In situ perfusion in rodents to explore intestinal drug absorption: Challenges and opportunities. *International Journal of Pharmaceutics***478**, 665-681 (2015).

40 Chen, G., Min, X., Zhang, Q., Zhang, Z. & Cheng, G. Synthesis and Evaluation of PEG-PR for Water Flux Correction in an In Situ Rat Perfusion Model. *Molecules***25**, 5123 (2020).

41 Hussain, N., Jaitley, V. & Florence, A. T. Recent advances in the understanding of uptake of microparticulates across the gastrointestinal lymphatics. *Advanced Drug Delivery Reviews***50**, 107-142 (2001).

42 Fojo, A. T. *et al.* Expression of a multidrug-resistance gene in human tumors and tissues. *Proc Natl Acad Sci U S A***84**, 265-269, doi:10.1073/pnas.84.1.265 (1987).

43 Cao, X. *et al.* Why is it challenging to predict intestinal drug absorption and oral bioavailability in human using rat model. *Pharm Res***23**, 1675-1686, doi:10.1007/s11095-006-9041-2 (2006).

44 des Rieux, A., Fievez, V., Garinot, M., Schneider, Y. J. & Préat, V. Nanoparticles as potential oral delivery systems of proteins and vaccines: a mechanistic approach. *J Control Release***116**, 1-27, doi:10.1016/j.jconrel.2006.08.013 (2006).

45 Gao, L. *et al.* Drug nanocrystals: In vivo performances. *J Control Release***160**, 418-430, doi:10.1016/j.jconrel.2012.03.013 (2012).

Figures

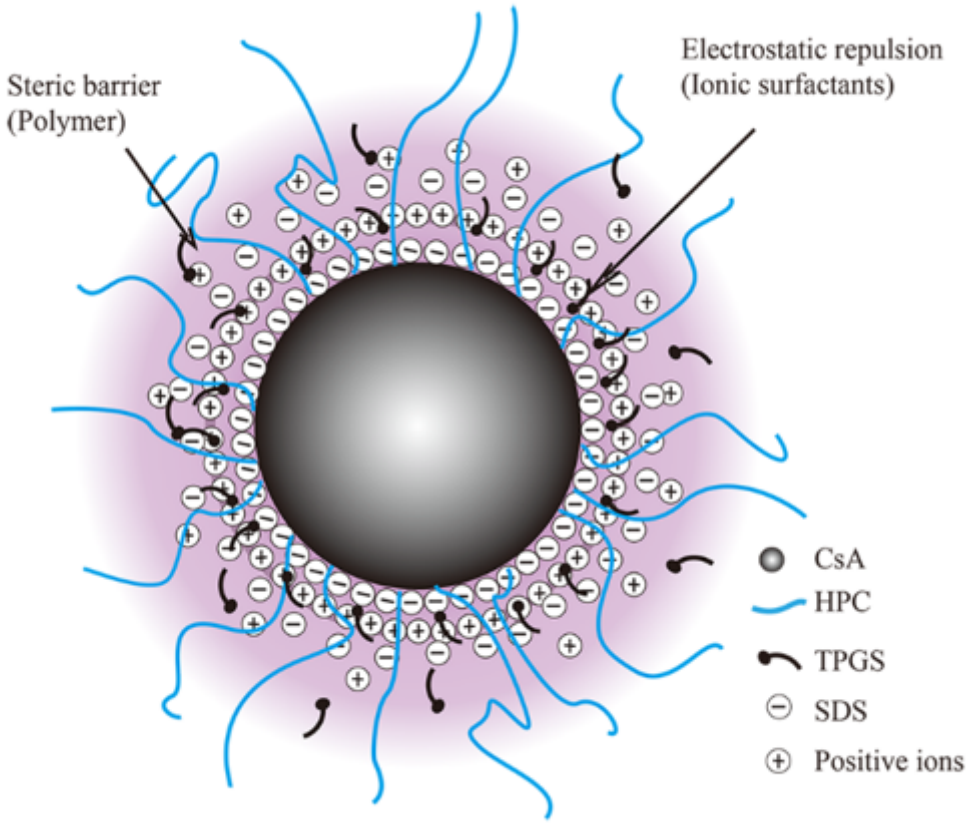

Figure 1

Structure scheme of CsA-NS.

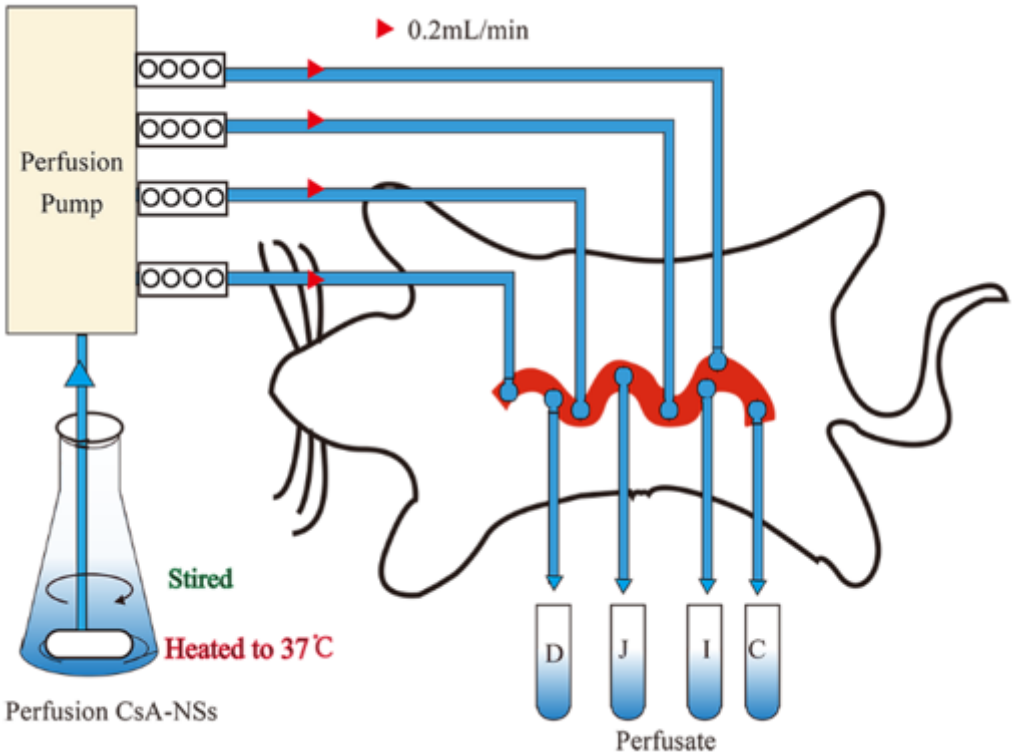

Figure 2

Four-site simultaneous perfusion model of rat intestine. D: Perfusate from duodenum; J: Perfusate from jejunum; I: Perfusate from ileum; C: Perfusate from colon.

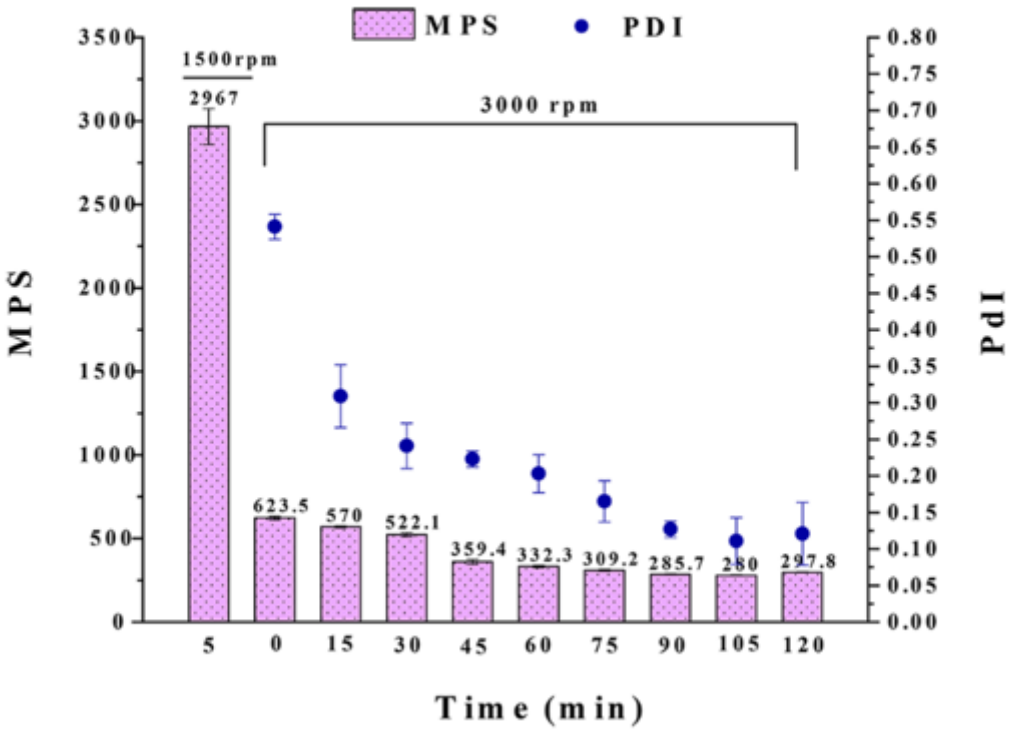

Figure 3

Mean particle size (MPS) and polydispesity index (PDI) as a function of milling time for cyclosporin A, (n = 3).

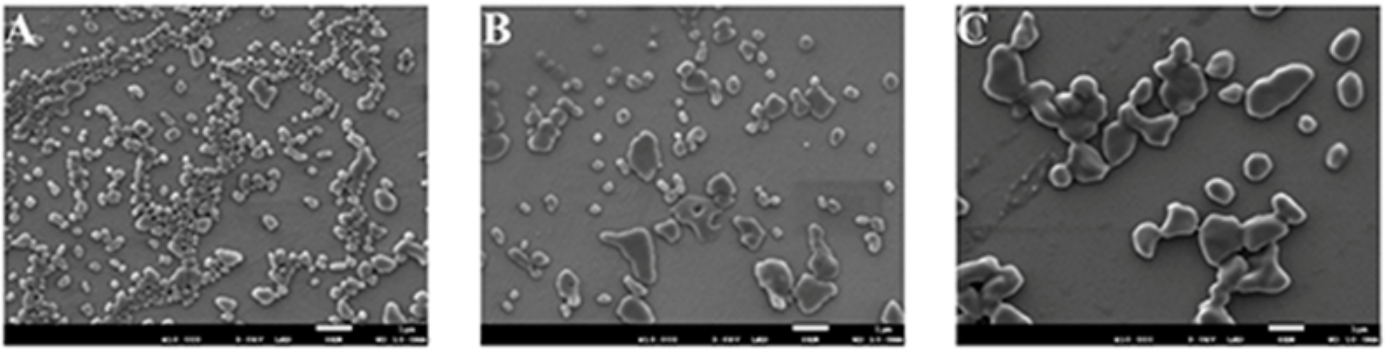

Figure 4

SEM of CsA -NSs of 280 nm (A), 522 nm (B), 2967 nm (C). Bar, 1 μm.

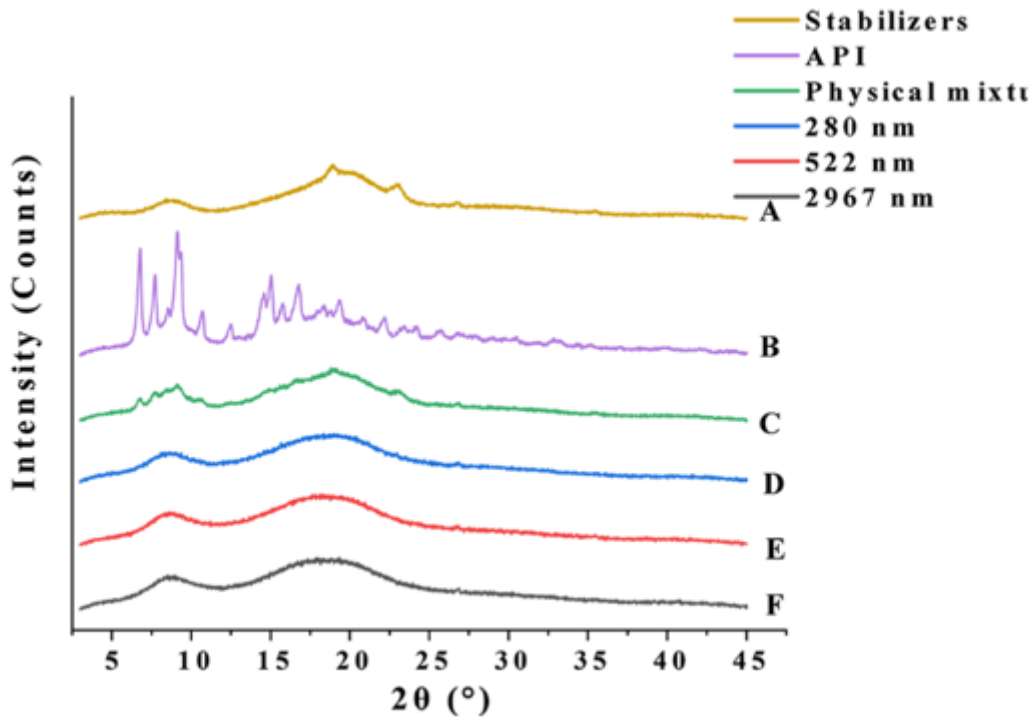

Figure 5

X-ray diffraction patterns of stabilizers (A), raw CsA (B), physical mixture(C), 280 nm (D), 522 nm (E), 2967 nm (F).

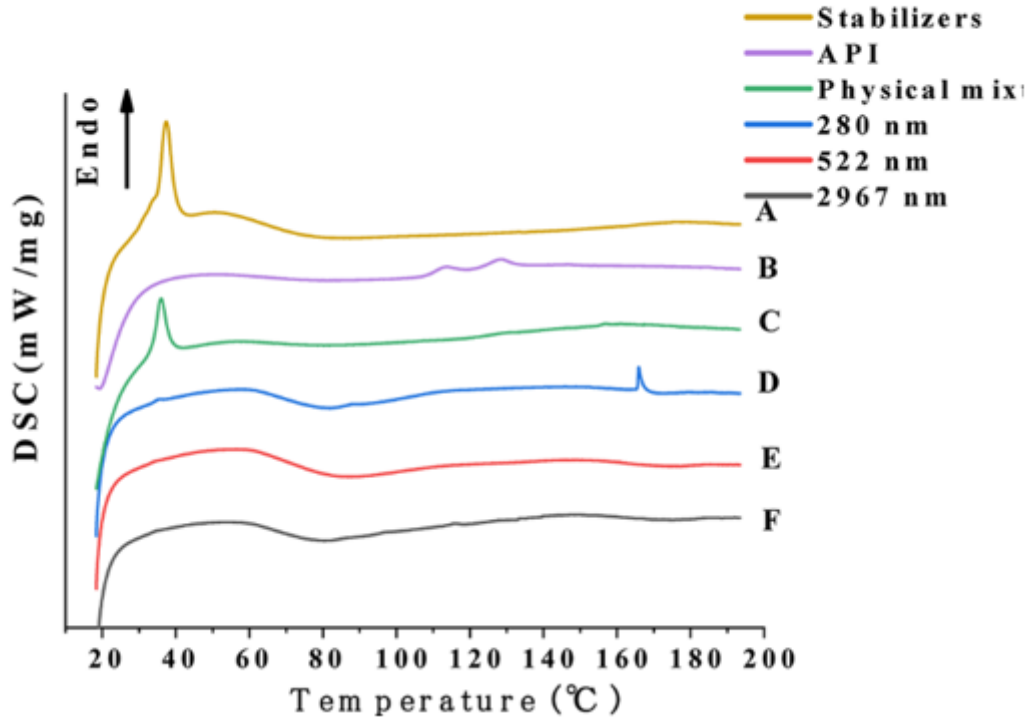

Figure 6

DSC diffraction patterns of stabilizers (A), raw CsA (B), physical mixture (C), 280 nm (D), 522 nm (E), 2967 nm (F).

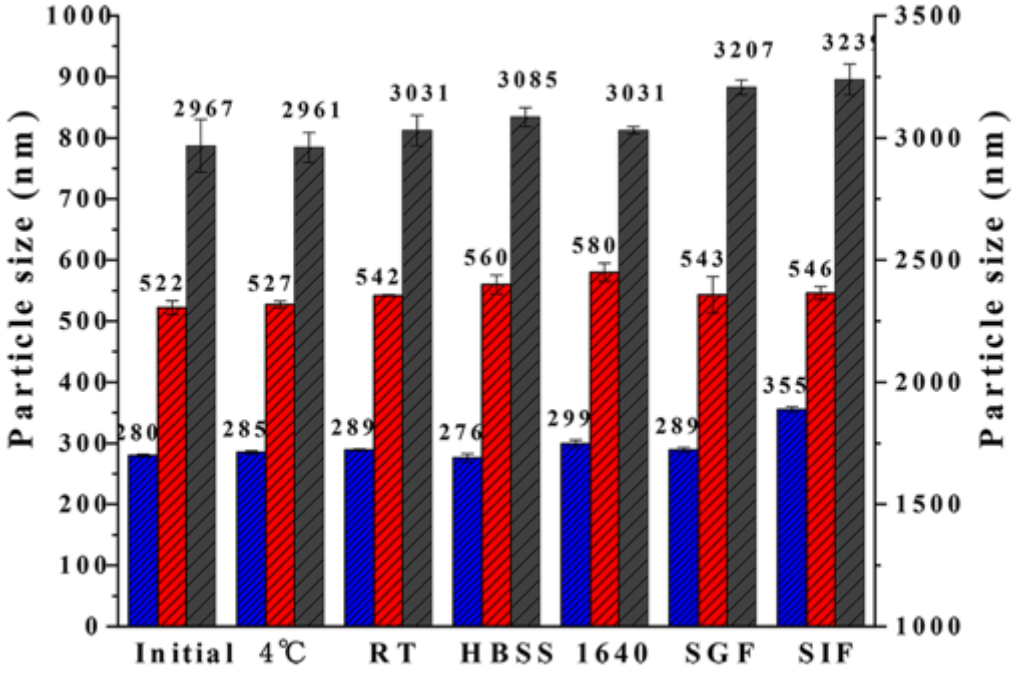

Figure 7

Particle size stability of CsA-NSs in different condition. Initial: 0 day after preparation; 4 ℃: stored at 4 °C for 3 months; RT: stored at room temperature for 3 months; HBSS: mixed with HBSS at 37 ℃ for 4 h; 1640: mixed with 1640 medium at 37 ℃ for 4 h; SGF: mixed with SGF at 37 ℃ for 2 h; SIF: mixed with SIF at 37 ℃ for 12 h, (n = 3).

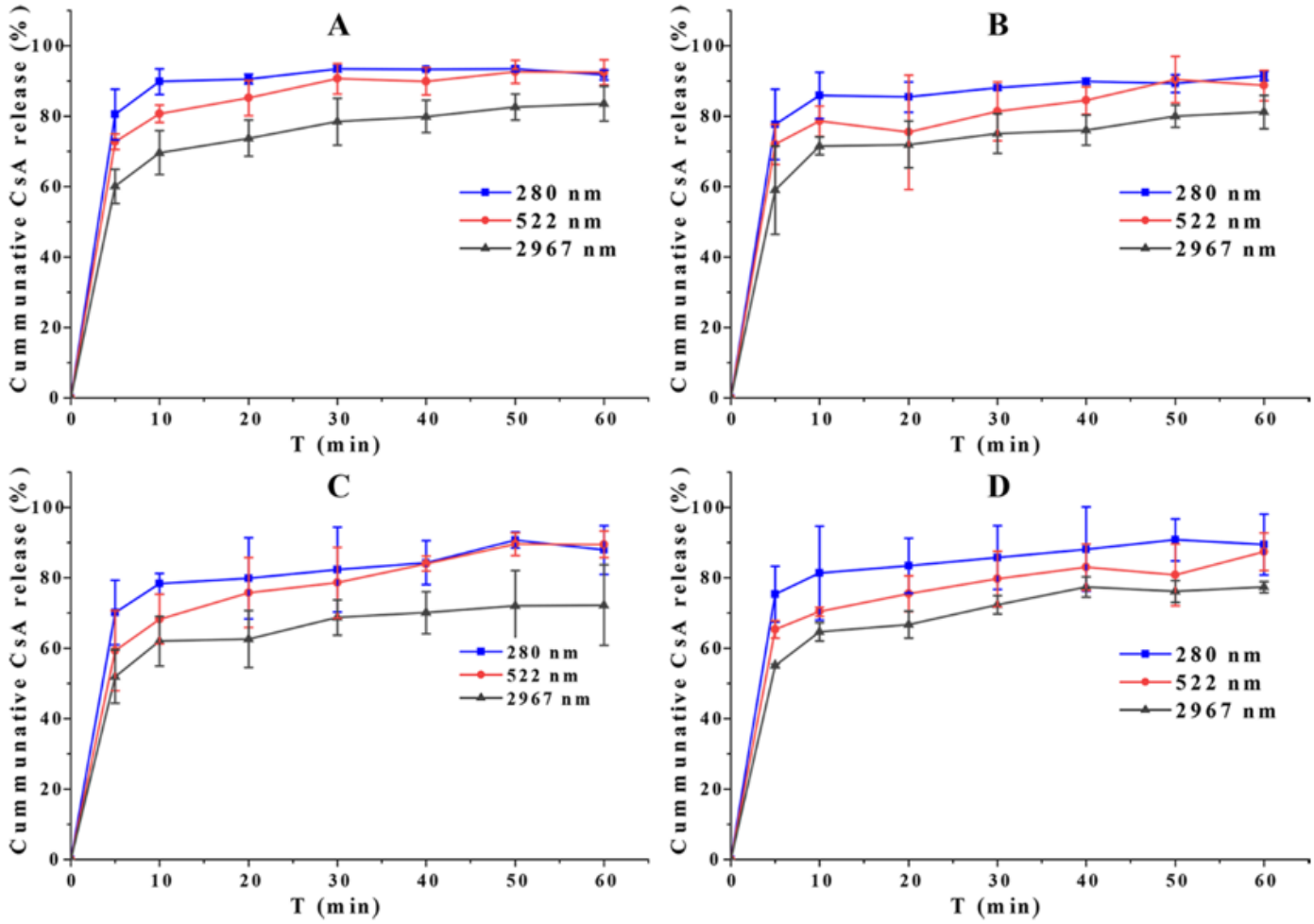

Figure 8

In vitro drug release testing of different sized (280 nm, 522 nm, and 2967 nm) nanosuspensions in water (A), pH 1.2, hydrochloric acid (B), pH 4.5, phosphate buffer (C) and pH 4.5, phosphate buffer (D). (USP apparatus II with paddles at 100 rpm, n = 3).

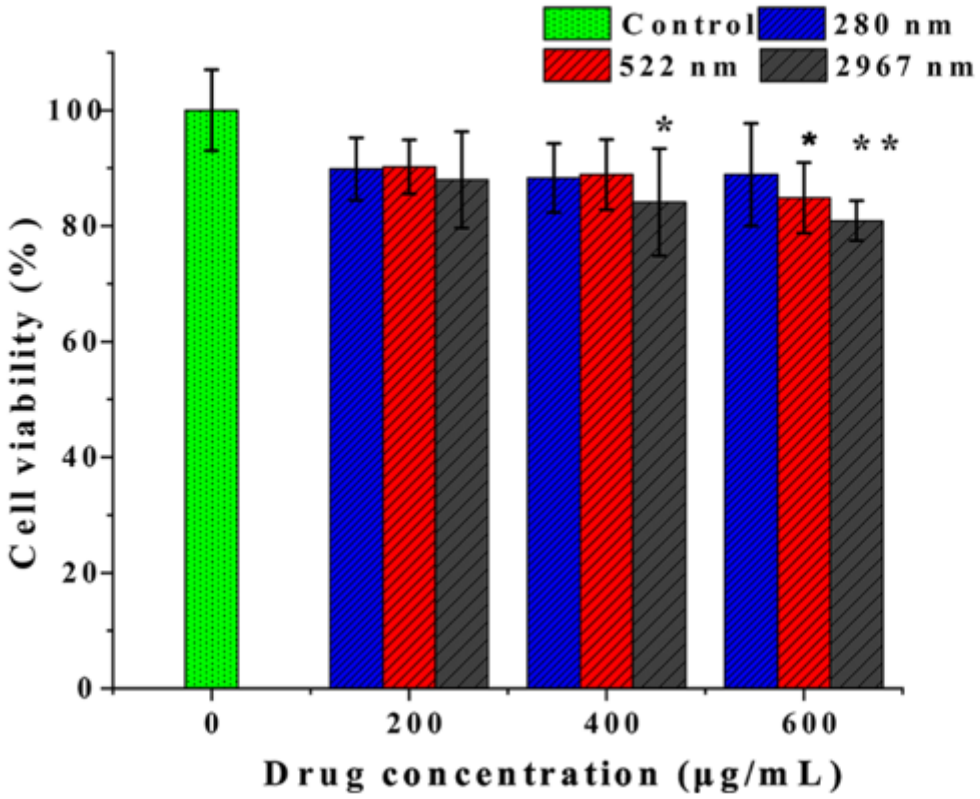

Figure 9

Cytotoxicity of Caco-2 cells treated with CsA-NSs at 4 h (n = 5), * represent significantly different compared with control ($p < 0.05$), ** represent extremely significant different compared with control ($p < 0.01$).

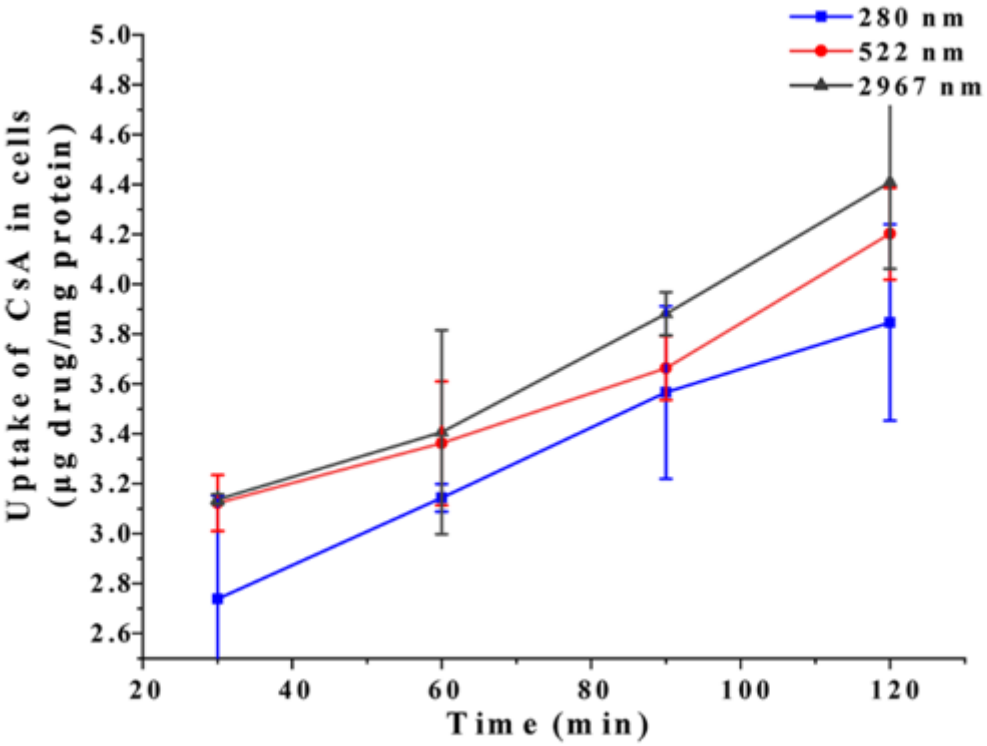

Figure 10

Cellular uptakes of different sized CsA-NSs into Caco-2 cells (40 μg/mL CsA) (n = 3).

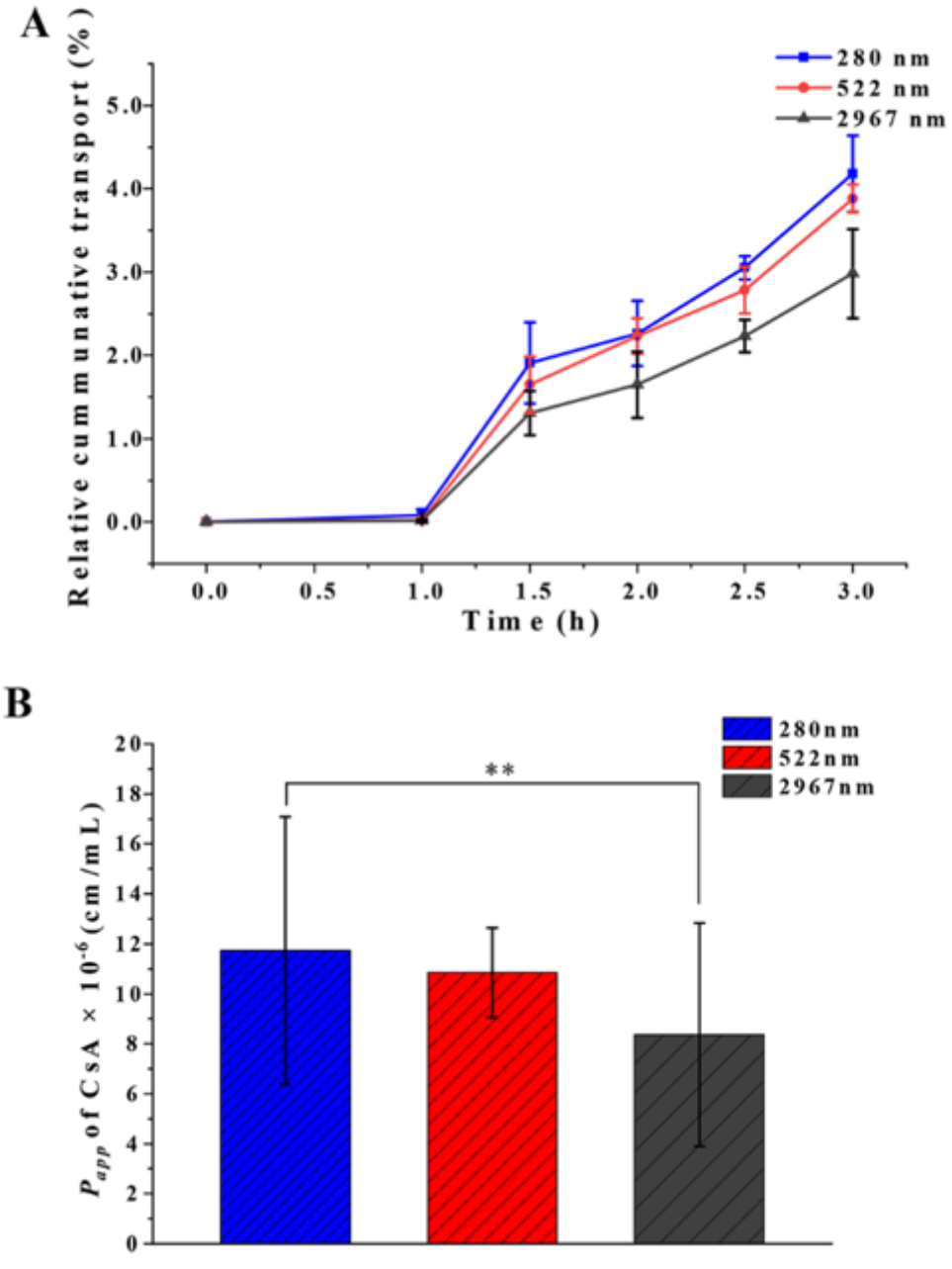

Figure 11

(A) Relative cumulative transport of CsA in CsA-NSs across Caco-2 monolayer; (B) Apparent permeability coefficient (Papp) of CsA across a Caco-2 cell monolayer (n = 3). ** represent extremely significant different compared with control ($p < 0.01$).

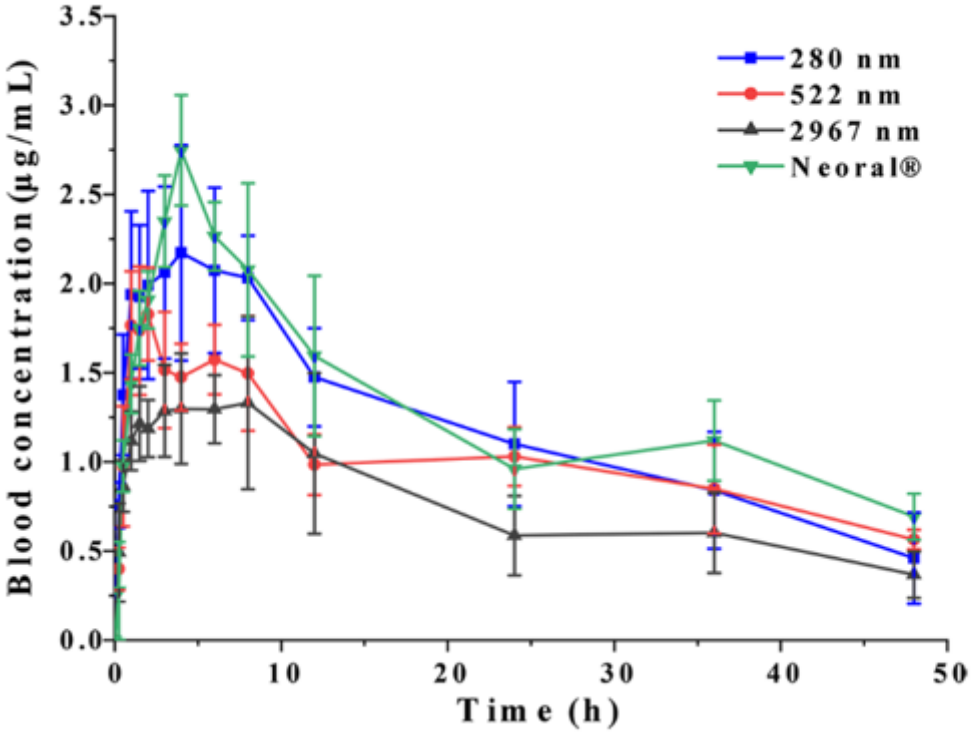

Figure 12

Mean drug blood concentration-time profiles after oral of Neoral® and CsA-NSs at a dose of 25 mg/kg in S.D. rats (n = 5, means ±s).

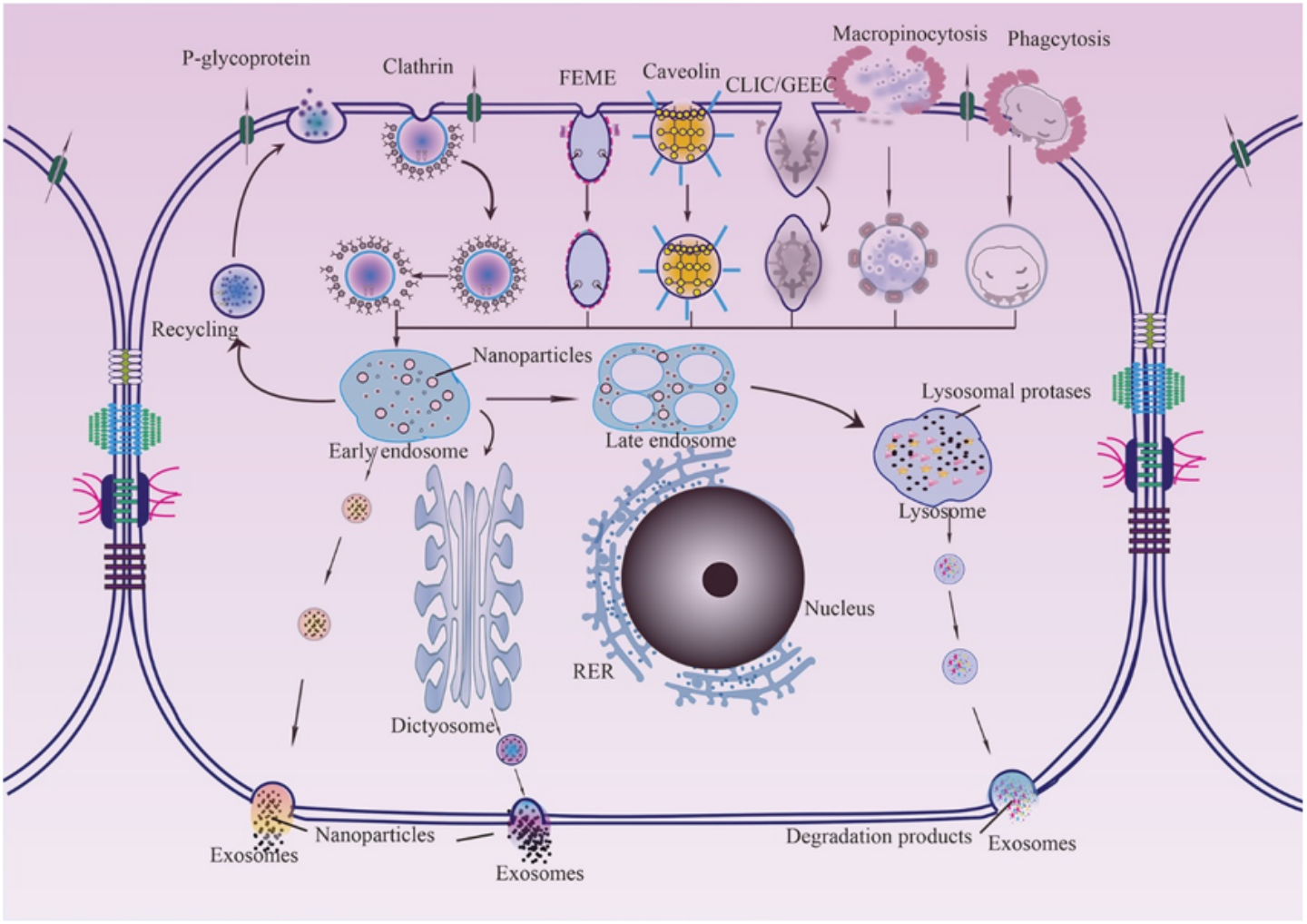

Figure 13

Schematic diagram about cellular uptakes of CsA-NSs into Caco-2 cells. FEME: clathrin-independent/dynamin-dependent endocytosis; CLIC/GEEC: clathrin-independent/dynamin-independent endocytosis; RER: rough endoplasmic reticulum.

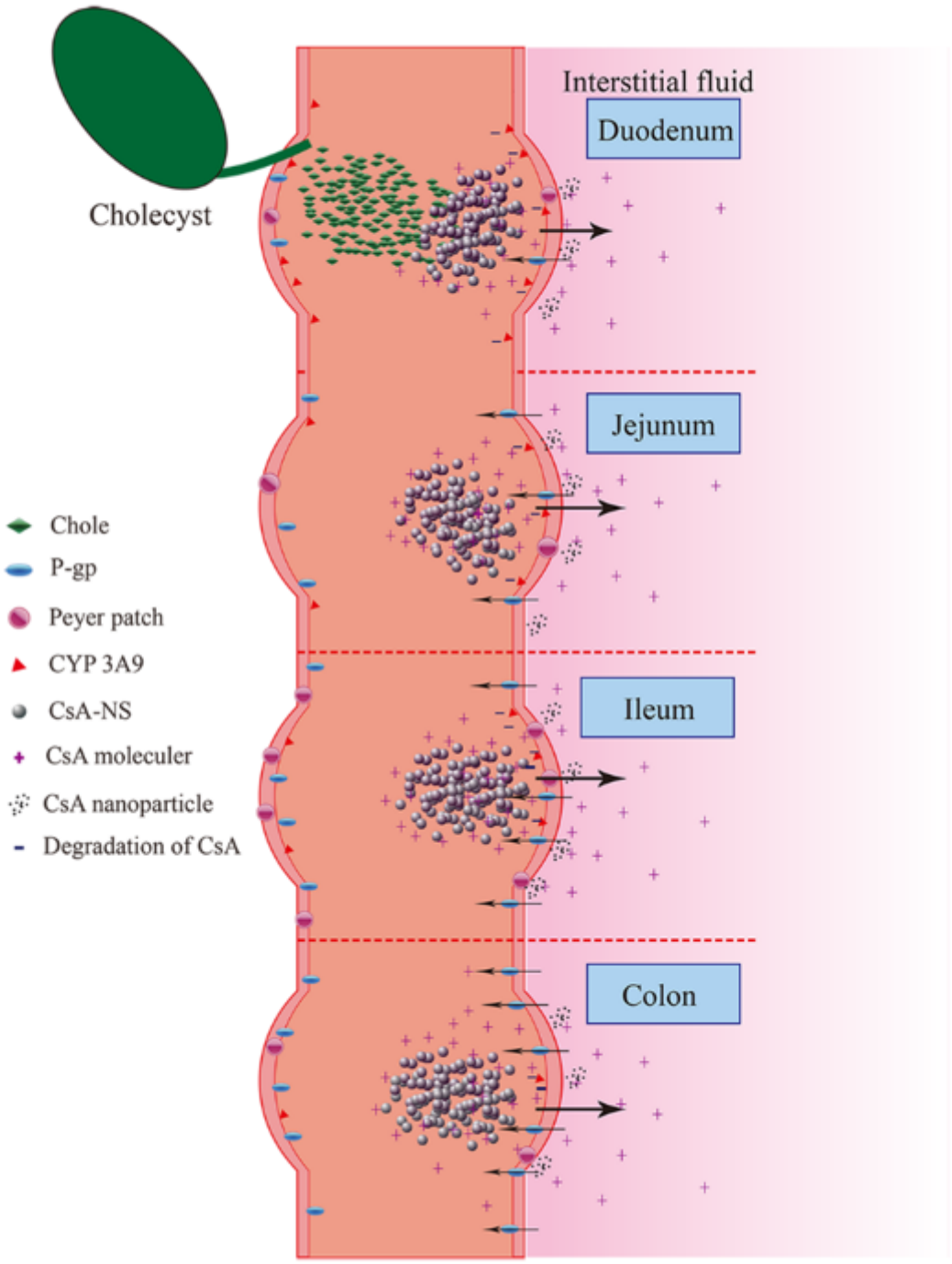

Figure 14

Schematic diagram about transport of CsA-NSs in rat small intestine.

Supplementary Files

This is a list of supplementary files associated with this preprint. Click to download.

- GraphicalAbstract.docx

- Supplementarymaterial.docx